ROYAL SOCIETY OF CHEMISTRY

PAPER

Check for updates

A novel potentiometric sensor based on ZnO decorated polyaniline/coal nanocomposite for diltiazem determination

G. A. El Sayed,[a] Mostafa R. Abukhadra, [ID][b] S. M. Mostafa,[a] M. Rabia,[c] Mohamed Ali Korany[a] and M. M. Khalil [ID] *[a]

Diltiazem (DTZ) is one of the most effective medications for treating cardiovascular diseases. It has been widely used for the treatment of angina pectoris, hypertension and some types of arrhythmia. The development and application of a modified carbon paste sensor with improved detection limits for the potentiometric determination of diltiazem are the main goals of the current study. Sensitivity, long-term stability, reproducibility and improving the electrochemical performance are among the characteristics that have undergone careful examination. A modified carbon paste sensor based on β-cyclodextrin (β-CD) as ionophore, a lipophilic anionic additive (NaTPB) and a ZnO-decorated polyaniline/coal nanocomposite (ZnO@PANI/C) dissolved in dibutyl phthalate plasticizer, exhibited the best performance and Nernstian slope. The ZnO@PANI/C based sensor succeeded in lowering the detection limit to 5.0×10^{-7} through the linear range 1.0×10^{-6} to 1.0×10^{-2} mol L^{-1} with fast response time ≤ 10.0 s. The prepared nanomaterial was characterized using X-ray diffraction (XRD), Fourier transform infrared (FT-IR) spectroscopy and scanning electron microscopy (SEM). The surface properties of the proposed sensor were characterized by electrochemical impedance spectroscopy (EIS). The selectivity behavior of the investigated sensor was tested against a drug with similar chemical structure and biologically important blood electrolytes (Na$^+$, K$^+$, Mg^{2+}, and Ca^{2+}). The proposed analytical method was applied for DTZ analysis in pure drug, pharmaceutical products and industrial water samples with excellent recovery data.

1. Introduction

The public health problem of hypertension is widespread throughout the world. It is acknowledged as the main modifiable risk factor for cardiovascular diseases (CVDs), causing substantial annual economic and health costs. It is a significant contributor to coronary heart disease, heart failure, potential hemorrhagic stroke, peripheral vascular disease, renal impairment, retinal hemorrhage, and visual impairment.[1] Diltiazem, [[(2S-cis)-3-(acetyloxy)-5-[2-(dimethylamino)ethyl]-2,3-dihydro-2-(4-methoxyphenyl)-1,5-benzothiazepin-4(5H)-one] (Fig. 1), is one of the medications in the class called calcium-channel blockers and is among the most commonly used agents for hypertension and angina. Diltiazem (DTZ) works by preventing calcium ions from entering the heart. Reduced intracellular calcium concentrations result in more relaxed smooth muscles, which dilate the blood vessels and lower blood pressure.[2] As a result, it is essential to

closely monitor the DTZ level in pharmaceutical doses and biological fluids when using this medication. It has been reported that DTZ can be detected in its solutions using a variety of analytical techniques, including high performance liquid chromatography (HPLC),[3] gas chromatography,[4] high performance thin layer chromatography (HPTLC),[5] spectrophotometry,[6] voltammetry[7–9] and potentiometry.[10] Most of the aforementioned techniques have plenty of limitations, including the requirement for expensive equipment, the need for earlier time-consuming treatment or derivatization reactions and their inapplicability to colored and turbid drug sample solutions. Potentiometric sensors, on the other hand, are an innovative and successful analytical technique known to overcome most of these deficiencies. Fast-stable response, low cost, ease of preparation and application, flexibility and the ability to be miniaturized make this measurement technique a desirable option with additional favorable advantages. Carbon paste sensors (CPS) play an important role in drug detection and these kinds of sensors have many advantages over other types including significant potential stability, ease of manufacturing and simplicity. These developed sensors have the potential to be applied to provide quick analysis, rapid responses, excellent selectivity, and inexpensive analysis.[11–13] All of these merits make potentiometric approaches the most favorable approach for DTZ assessment. Nanomaterials exhibit

[a]Chemistry Department, Faculty of Science, Beni-Suef University, Beni-Suef, Egypt. E-mail: magdy_mmagdy@yahoo.com; mohamed.mahmoud@science.bsu.edu.eg

[b]Materials Technologies and their Applications Lab, Geology Department, Faculty of Science, Beni-Suef University, Beni-Suef, Egypt

[c]Nanomaterials Science Research Laboratory, Chemistry Department, Faculty of Science, Beni-Suef University, Beni-Suef, 62514, Egypt

improved properties that are not observable in bulk materials. When nanostructures are a part of the recognition layer, their incredibly high surface-to-volume ratio promotes a greater interaction with the target ions. Additionally, when using nanomaterials as the transducing constituents of potentiometric sensors, the exceptional electrical properties, such as the high charge transfer and the extraordinary electrical capacities generated at the interfaces of some nanostructured materials, are of crucial importance. Conjugated conductive polymers principally involve polyaniline (PANI), polythiophene (PTH), polypyrrole (PPY), and their products.[14] They have a wide range of potential applications, including microwave absorption, gas separation membranes, chemical sensors, rechargeable battery, photovoltaic cell, electromagnetic interference shielding, and more.[15] Additionally, conductive polymers are utilized, such as conducting fillers in insulating polymer substrates to acquire conducting polymer compounds. These materials could be used as sensors for display devices, electronic equipment, and electromagnetic interference shields.[16] ZnO is one of the most likeable materials because of its simple synthesis, lack of toxicity, notable optoelectronic properties, high stability and low cost. Recently, several techniques were developed to enhance the performances and physicochemical properties of ZnO as vital materials in several applications involving the metallic doping of its structure, integration in composites and heterojunction structures as well as the supporting of its particles into suitable carriers.[17] However, numerous studies have assessed the application of synthetic carbon-based substrates (graphene and CNTs) to induce the physicochemical performance of ZnO. These structures are still expensive, require complicated production processes and lack natural availability. Natural coal as a substrate can provide an effective alternative for such structures. Coal is a highly affordable, readily available and reactive structure composed of aromatic polycyclic hydrocarbons that are saturated with numerous active oxygenated chemical groups.[18–20] It was expected that the functionalization of coal by conducting polymers as polyaniline can result in promising substrate of significant enhancement impact on the properties of the supported ZnO particles.

Polyaniline is a widely used conductive polymer that exhibits a high surface area, significant stability, is non-toxic and is a cost-effective polymer.[21,22] The integration of PANI with additional semiconductors may improve the charge carrier transfer performance at the semiconductor–PANI interfaces.[23] The enhanced separation of photogenerated charge carriers is due to the better
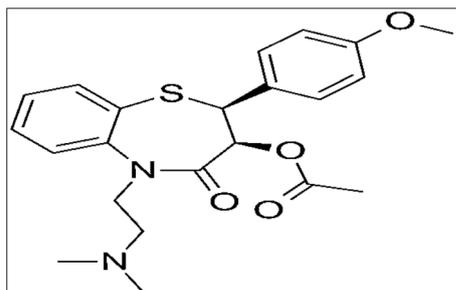
Table 1 Proximate and ultimate analysis of the original coal sample

Constituent	Wt%
Proximate analysis	
Moisture	2.41
Volatile matter	50.49
Ash	6.50
Fixed carbon	40.6
Ultimate analysis	
Carbon	68.4
Nitrogen	2.53
Oxygen	10.6
Hydrogen	6.30
Sulfur	2.32

charge carrier mobility of PANI. The potential enhancement of the electrical, optical, and dielectric characteristics of polyaniline blends can be accomplished through the synergistic interaction of tunable functions shown by inorganic as well as organic nanoparticles of semiconductors.[24,25] Therefore, it was predicted that the combination of ZnO nanoparticles and polyaniline/coal composites as substrates would result in considerable improvement in the doping level and stability of the composite structure.

Therefore, the presented study implemented the fabrication of new hybrid structures of ZnO-decorated polyaniline/coal nanocomposite (ZnO@PANI/C) by facile technique as a novel, highly effective, low-cost and accessible potentiometric sensor to accurately determine DTZ in its pure form, dosage form, biological fluids (urine), and industrial water samples. ZnO@PANI/C nanocomposite was characterized using XRD, FT-IR, and SEM. The sensor showed good sensitivity, adequate selectivity, and high thermal stability for DTZ determination.

2. Experimental

2.1 Reagents and materials

All chemicals utilized in this study were of analytical grade. Deionized water was used throughout all experiments. Pure DTZ was provided by EIPICO, Egypt. The pharmaceutical formulation (ALTIAZEM®) was purchased from local drug stores. Verapamil hydrochloride was given by Abbott, Cairo,
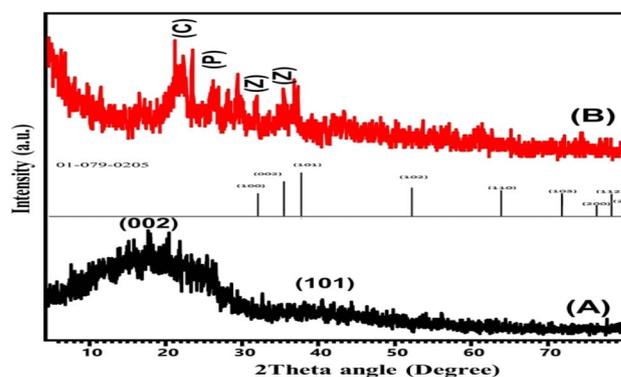

Fig. 1 Chemical structure of DTZ.

Fig. 2 XRD patterns of raw coal (A) and synthetic ZnO@PANI/C (B) (C: coal; Z: ZnO; P: polyaniline).
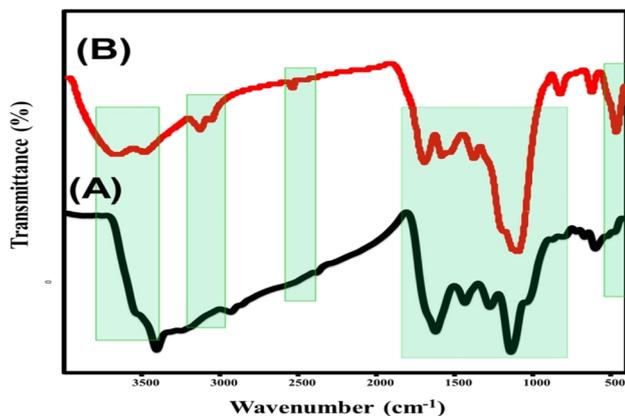
Fig. 3 FT-IR spectra of raw coal (A) and synthetic ZnO@PANI/C (B).

Egypt. Spectroscopic graphite powder (1–2 mm) was purchased from Sigma-Aldrich. Dioctyl adipate (DOA) and sodium tetraphenylborate (NaTPB) were obtained from Fluka (USA). Dibutyl phthalate (DBP), dioctyl phthalate (DOP) and dioctyl sebacate (DOS) were purchased from Merck (Germany). 18-Crown-6 and β-cyclodextrin (β-CD) were purchased from Euromedex, France. The metal salts were provided by BDH (UK) as nitrates or chlorides. Low to medium-grade high volatile bituminous coal was supplied by El-Maghara coal mine; in Sinai Egypt (Table 1). Aniline monomers (C_6H_7N), ammonium persulphate $(NH_4)_2S_2O_8$, sodium hydroxide pellets NaOH, hydrochloric acid HCl, methanol, ethanol and zinc nitrate hexahydrate $Zn(NO_3)_2 \cdot 6H_2O$ were procured from Sigma-Aldrich Company, Egypt. Standard solution of 1.0×10^{-2} mol L^{-1} DTZ was freshly prepared by dissolving the accurately weighed amount in deionized water. Working solutions (1.0×10^{-7} to 1.0×10^{-2} mol L^{-1}) of the drug were prepared. Concentrated solutions of NaOH and HCl were used within the range (0.1–1.0 mol L^{-1}) for adjusting pH of the medium.

2.2 Synthesis of ZnO decorated polyaniline/coal nanocomposite (ZnO@PANI/C)

Simple hydrothermal synthesis procedures allowed for the decoration of raw coal with sub-bituminous coal. Firstly, 5.0 g of the ground raw coals were dispersed within 100.0 mL of deionized water under vigorous stirring for 10.0 minutes to obtain homogenous slurry. The obtained slurry was supplemented with 5.0 g of zinc nitrate salt and stirred for an additional 15.0 minutes to ensure the complete dissolving of the zinc-bearing salt. Afterward, the obtained mixture was treated with NaOH solution (1.0 mol L^{-1}) under continuous stirring for about 12.0 h. After that, the decorated product was extracted from the residual solutions by centrifugation for 15.0 minutes at 300.0 rpm. Then the sample was thermally treated in inert conditions for 5.0 h at 350.0 °C obtaining a ZnO/coal composite (ZnO/C).

The integration between the prepared ZnO/C particles and the polyaniline polymer was accomplished according to the reported method by Sayed *et al.*[23] An aniline solution was prepared by direct dissolving of the aniline monomer (0.1 mol L^{-1}) in hydrochloric acid (0.5 mol L^{-1}) under the impact of sonication waves. The synthetic ZnO/C particles (1.0 g) were then dispersed homogenously within the aniline solution under the impact of both the stirring and sonication irradiation. Afterward, the oxidation reagent $(NH_4)_2S_2O_8$ (0.15 mol L^{-1}) was added suddenly to the mixture, which was subjected to the sonication treatment for 1 h followed by continuous stirring for 24.0 h at the room temperature (28 °C) to ensure the polymerization reactions. Then the formed composite was separated using a centrifuge, washed carefully, and dried overnight at 50.0 °C. The product was labeled as ZnO@PANI/C and was kept for further characterization and applications.

2.3 Equipment

Metrohm 702 SM Titrino (Metrohm, Switzerland) was used for potentiometric and pH-measurements. Based on the obtained XRD patterns, the crystallinity, and the main crystal phases had been determined using a PANalytical-Empyrean X-ray diffractometer across a detection range of 0.0 to 70.0 °C. A Fourier transform infrared spectrometer (FTIR8400S; Shimadzu) was used to discriminate between the chemical compositions of ZnO@PANI/C within the determination frequency range of 400.0 cm^{-1} to 4000.0 cm^{-1}. SEM images were captured by a scanning electron microscope (Gemini, Zeiss Ultra 55) immediately after coating the ZnO@PANI/C particles with thin
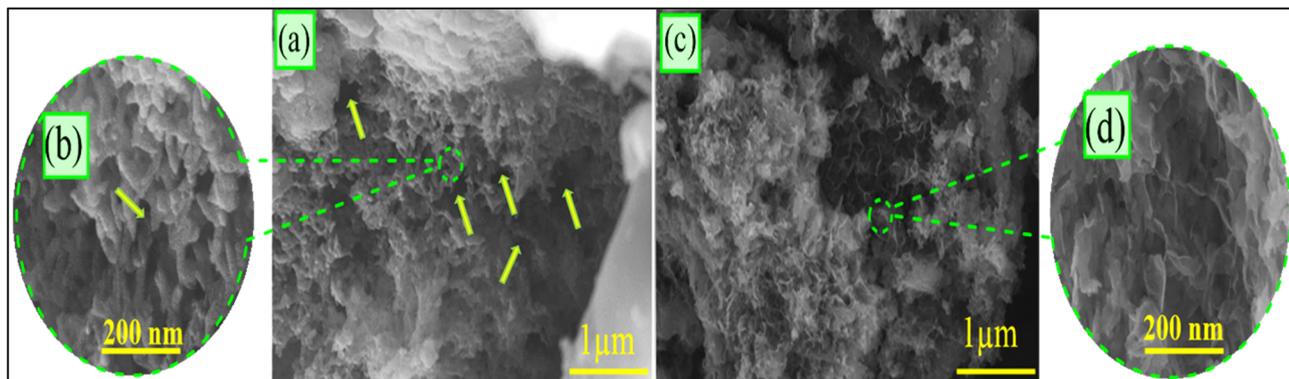

Fig. 4 SEM images of the synthetic ZnO@PANI/C with declaration of the integrated polyaniline (a and b) and the decorated ZnO (c and d).
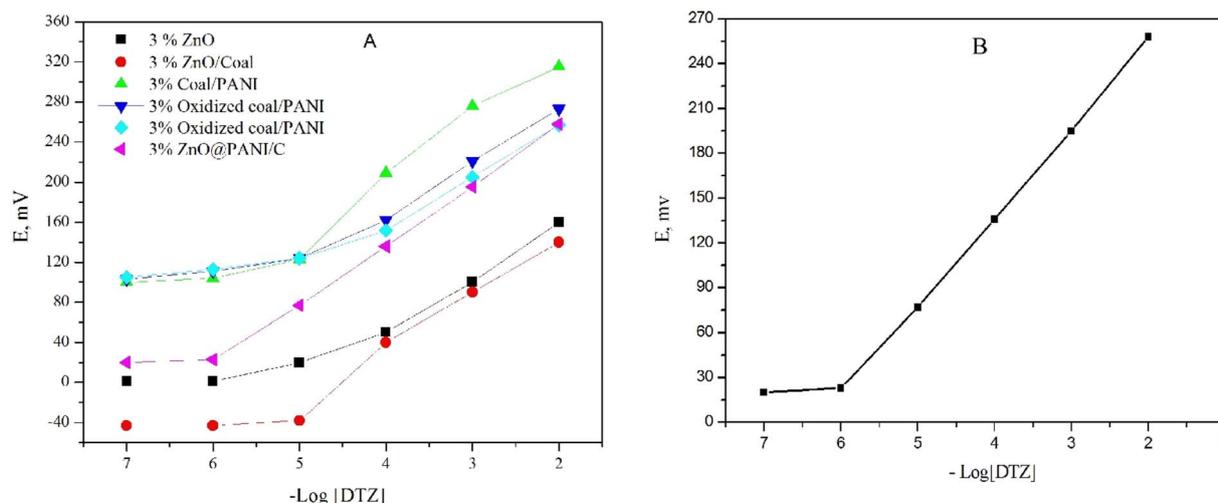
Fig. 5 Calibration curves of (A) different nanomaterials, (B) DTZ-CPS at optimum paste composition.

gold films. The HRTEM images, which were produced using a transmission electron microscope (JEOL-JEM2100) at an accelerating voltage of 200 kV, have been used to study the internal structure of ZnO@PANI/C.

2.4 Sensors construction

The proposed sensor was created utilizing techniques that have been previously described.[11] In a Petri dish, different proportions of β-CD ionophore, NaTPB as a lipophilic anionic additive, ZnO@PANI/C nanocomposite and spectroscopic graphite powder/plasticizers (50.0/50.0%) were mixed together to create a smoothly wet paste. This paste was packed inside the tip of a polypropylene sensor body. On a piece of smooth paper, the paste was polished to acquire a shiny surface. After soaking for 30.0 minutes in a solution containing 1.0×10^{-3} mol L^{-1} DTZ, the constructed sensor is used for potentiometric measurements.

3. Results and discussion

3.1 Characterization of the nanocomposite

The obtained X-ray diffraction patterns of raw coal as well as the synthetic ZnO@PANI/C structure that was applied in the production of the detection electrode are presented in Fig. 2.

The diffraction pattern of raw coal shows the characteristic peaks of amorphous carbonaceous materials with their noticeable broad peaks (8.0°–30.0° (002) and 40.0°–50.0° (101)).[23] The recognized diffraction pattern of ZnO@PANI/C demonstrates significant interaction between the integrated components, with obvious indications about the essential components of the composite. The decorated ZnO particles were identified by highly reduced and shifted diffraction peaks of wurtzite ZnO (31.72° (100), 34.45° (002), 36.3° (101), 47.5° (102)). The remarkable shifting in the ZnO diffraction peaks declares the strong interaction with the polymeric chains of polyaniline or its coating with the polymeric matrix.[26] The integrated PANI structure was confirmed by its identification peak around 27.5° (200), which signify its semi-crystalline properties.[27]

The raw sample demonstrated the identification of the main chemical groups of natural coal. The essential chemical groups that were detected are carboxylic O–H groups or alcoholic O–H that results from hydrogen bonding in coal (3000.0 cm^{-1} to 3600.0 cm^{-1}), COOH groups (1716.0 cm^{-1}), asymmetric (2858.0 cm^{-1}) and symmetric (2940 cm^{-1}) vibrations of aliphatic C–H (sp^3), C–C aromatic stretching (1616.0 cm^{-1}), C–H vibration in the methylene group (1450.0 cm^{-1}), C–H vibration in the methyl group (1372.0 cm^{-1}), C–O stretching (1000.0–1200.0 cm^{-1}), and aromatic C–H bending vibrations

Table 2 Response characterization of the proposed sensor

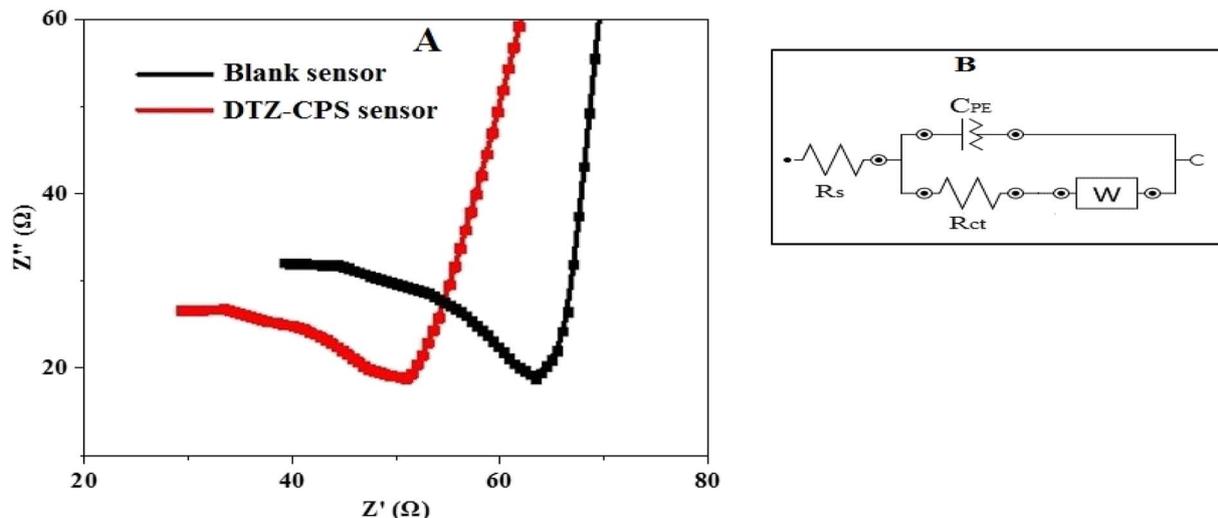| Parameter	DTZ-CPS
Composition	0.50% β-CD + 0.50% NaTPB + 3.0% ZnO@PANI/C + 46.5% graphite + 49.5% DBP
Slope (mV per decade)	62.0 ± 0.9
Correlation coefficient (r^2)	0.994
Detection limit (mol L^{-1})	5.0×10^{-7}
Quantification limit (mol L^{-1})	1.6×10^{-6}
Concentration range (mol L^{-1})	1.0×10^{-6} to 1.0×10^{-2}
Response time (s)	≤ 10
RSD (%)	1.45
Isothermal coefficient (mV per °C)	0.0053

Fig. 6 (A) EIS of the synthesized DTZ-CPS sensor against the blank sensor and (B) equivalent circuit.

$(500.0–900.0 \text{ cm}^{-1})$.[23,28] Regarding the obtained FT-IR spectrum of ZnO@PANI/C, the observed spectrum exhibits the characteristic absorption bands of raw coal but at slightly deviated positions, in addition to some new bands related to the integrated polyaniline polymer and ZnO. The characteristic band of Zn–O was identified at about 480 cm^{-1}.[29] Additionally, the marked bands around 1590.0 and 1450.0 cm^{-1} at the studied spectrum of ZnO@PANI/C were assigned to the C=C stretching deformation of the quinoid and benzenoid rings in the polyaniline polymer, respectively.[26,30] In addition to other identification bands of polyaniline around 2350.0 cm^{-1} (C≡N) as well as 1295.0 and 1130.0 cm^{-1} (C–N of secondary aromatic amine) were observed in the spectrum of the composite[26,27] (Fig. 3).

The SEM images of the synthetic ZnO@PANI/C display a strong coating of the coal-layered particles with the polyaniline polymer (Fig. 4). The polyaniline polymer was detected clearly with its intersected nanorods, which give the surface of the coal a porous surface of secondary pores and rugged topography, which significantly increases its surface area. Moreover, the decorated ZnO nanoparticles appeared as intersected bended flakes in honeycomb structures, which are common for the synthesis of ZnO in the presence of an organic or polymeric substrate.

3.2 Optimization of the sensor matrix

A comprehensive study of the composition of the sensing matrix, including the type and quantity of the sensing ionophore, anionic additives, plasticizer, and nanomaterials, was carried out to achieve the highest performance. Ionophores are considered to be the most important sensing components in potentiometric sensors. They have the ability to form stable host–guest inclusion complexes with high molecular selectivity.[31] The preliminary study showed that the fabricated sensor without electroactive materials showed low potentiometric response and barely selectivity toward the target drug cation. Gradually, the incorporation of different amounts of β-CD as

sensing ionophore showed enhancing in the sensors performance. The addition of 0.5% (w/w) β-CD to the paste composition improve the Nernstian slope to 43.6 ± 0.9 mV per decade, concentration range 1.0×10^{-5} to 1.0×10^{-2} mol L^{-1} and detection limit 1.5×10^{-6} mol L^{-1}. However, the extra increase of the ionophore percentage above 0.5%, the paste becomes turbid and the sensors' potential response struggles.

Lipophilic anionic additives increase ionic mobility in the electrode matrix and the interfacial ion exchange kinetics at the electrode surface. The response of ISEs with ionic sites can tell whether an ionophore is acting as a neutral carrier. Whenever anionic sites are present, cyclodextrin as a neutral carrier ionophore performs its function. In order to decrease the ohmic resistance and improve the electrochemical properties of the potentiometric sensors, NaTPB is integrated as an anionic additive. The exchange kinetics at the sample–sensor interface
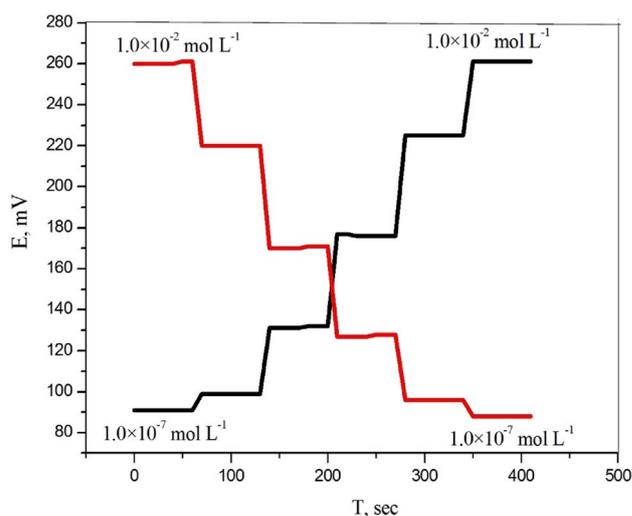

Fig. 7 The dynamic response time of CPS for step changes in concentrations of DTZ from low to high and *vice versa*.
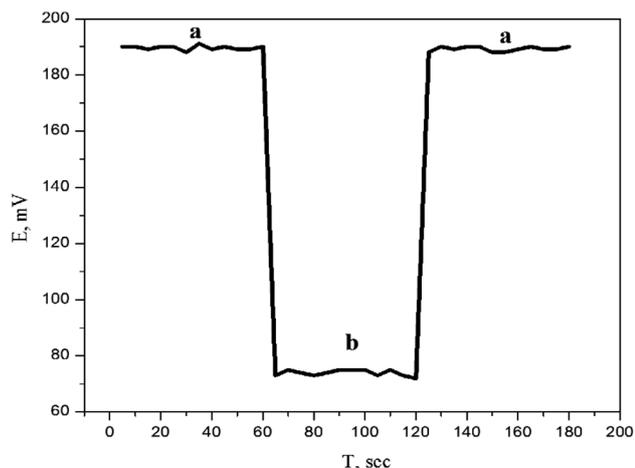
Fig. 8 Water layer test for the proposed sensor. Measurements were recorded in 1.0×10^{-3} mol L^{-1} DTZ (a) and 1.0×10^{-3} mol L^{-1} verapamil hydrochloride (b).

might also be accelerated.[32] A remarkable improvement (slope 55.0 ± 0.9 mV per decade, concentration range 1.0×10^{-6} to 1.0×10^{-2} mol L^{-1} and detection limit 1.0×10^{-6} mol L^{-1}) obtained by incorporating of 0.5% (w/w) NaTPB into the sensor paste. Further, lipophilic anionic additive has no impact on the sensor response.

Additionally, the incorporation of nanomaterials in the composition of the carbon paste directly affects the sensor's conductivity and increases the conversion of chemical signals into electrical signals. To enhance sensor performance, a family of different promising nanomaterials (C/PANI, oxidized coal/PANI, oxidized coal/activated PANI and ZnO@PANI/C) with a large surface area and sufficient absorptivity were chosen (Fig. 5(A)).

The results were monitored carefully in order to select the best nano-composite. The data revealed that, ZnO@PANI/C has a positive impact on the potentiometric behavior of the sensor than others (Fig. 5). The resealable enhancement in the sensors

performance is attributed to improving the sensor conductivity and increasing the transduction of the chemical signal to an electrical signal. In order to nominate the best composition, different percentages of the ZnO@PANI/C ranging from 1.0% to 10.0% (w/w relative to carbon powder) were added to the paste matrix containing 0.50% β-CD, 0.50% NaTPB, DPB plasticizer and graphite powder. The results in Table 2, indicated that the addition of 3.0% ZnO@PANI/C improved the Nernstian slope (62.0 ± 0.9 mV per decade), linear range (1.0×10^{-6} to 1.0×10^{-2} mol L^{-1}) and decreased the detection limit (5.0×10^{-7} mol L^{-1}). However, further increment in ZnO@PANI/C concentration led to deterioration of sensors performance. Finally, solvent mediator has a significant impact on the sensor performance; it plays a vital rule for solvation and distribution of the active components in the paste. Plasticizer helps controlling various equilibria between the ionophore and the primary ions in the paste phase hence improving performance of the sensor. Four synthetic plasticizers (DBP, DOS, DOP, and DOA) and a natural plasticizer (soybean oil) with different values of dielectric constants, lipophilicity and molecular weight were tested to figure out the one that shows the best response. The results showed that DBP plasticizer ($\varepsilon = 6.4$) shows a high potential reading, stability, distinguished potentiometric response and low detection limit compared with the other examined plasticizers. Therefore, DBP is used as a suitable plasticizer for the upcoming studies.

3.3 Electrochemical impedance spectroscopy (EIS)

The electrochemical impedance spectroscopy (EIS) results, as demonstrated in Fig. 6(A), illustrate the performance of the synthesized CPS sensor based on ZnO@PANI/C in comparison with a blank sensor. The EIS curves provide valuable insights into the sensor's superiority and this is particularly evident when examining the curve parameters. The electrical characteristics of the electrode/solution interface are realized by the equivalent circuit (Fig. 6(B)). In this circuit, the constant phase
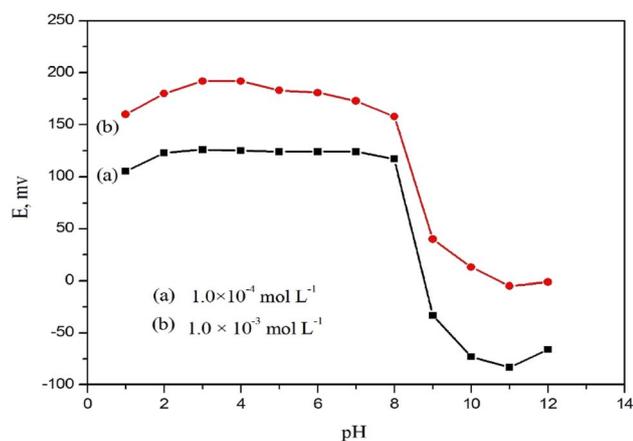

Fig. 9 Effect of pH of (a) 1.0×10^{-4} and (b) 1.0×10^{-3} mol L^{-1} DTZ solutions on the potential response of DTZ-CPS.
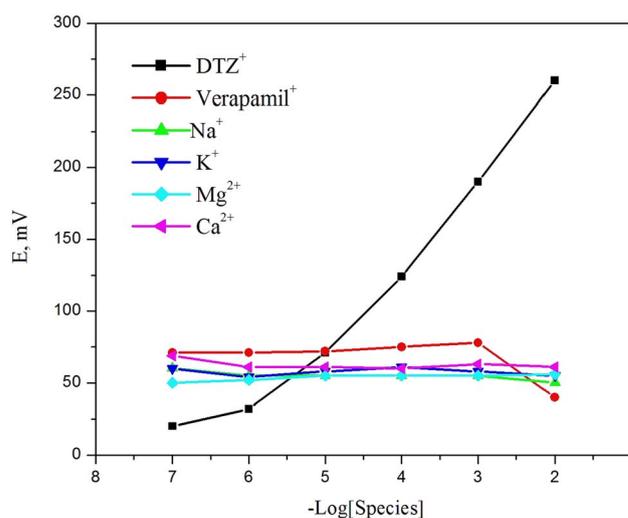

Fig. 10 Response to DTZ and some interfering species using DTZ-CPS.

Table 3 Application of the proposed sensor for the determination of DTZ in pure and pharmaceutical preparations and the statistical parameters

Sample	Statistical parameters	Standard addition method			Potentiometric titration method		
		Taken mg	Recovery (%)	RSD (%)	Taken mg	Recovery (%)	RSD (%)
Pure solution		0.23	101.00	0.92	13.53	102.30	1.2
		2.26	101.30	1.02	27.06	101.70	1.16
		22.55	100.00	0.97	40.59	101.10	1.22
	Mean $\pm$ SD		100.76 $\pm$ 0.9			101.7 $\pm$ 1.14	
	N		3			3	
	F-Ratio		1.6 (9.28)[a]				
	t-Test		1.8 (2.77)[b]				
Altiazem® (60 mg per tablet)		0.23	97.98	0.45		100.00	0.98
		2.26	98.92	0.61		98.33	0.93
		22.55	98.45	0.56		98.88	0.89
	Mean $\pm$ SD		98.45 $\pm$ 0.47			99.07 $\pm$ 0.85	
	N		3			3	
	F-Ratio		3.27 (9.20)[a]				
	t-Test		1.30 (2.77)[b]				

[a] Tabulated F-value at 95% confidence level. [b] Tabulated t-value at 95% confidence level and four degrees of freedom.

element (CPE), the diffusion (Warburg) impedance (W), the charge transfer resistance (R_{ct}) and the solution resistance of the electrolyte, between the working and the reference electrode (R_s). The semi-circuit values derived from the EIS data enable the precise calculation of R_s and R_{ct} for both the DTZ-CPS sensor and the blank sensor.[33] For the DTZ-CPS sensor, the R_s value stands at a low 28.0 Ω, while the R_{ct} value is even lower at 18 Ω. In contrast, the blank sensor exhibits slightly higher values, with R_s 38.0 Ω and R_{ct} 24.0 Ω. The significance of these findings lies in the small values of R_s and R_{ct} associated with the DTZ-CPS sensor. These low values indicate a highly efficient charge transfer process within the sensor, particularly for the detection of DTZ. In essence, the EIS analysis, as depicted in Fig. 6(A) serves as a compelling testament to the superior performance of the synthesized DTZ-CPS sensor. The calculated values of R_s and R_{ct}, notably lower than those of the blank sensor, underscore the sensor's excellent charge transfer capabilities, making it highly effective for the detection of DTZ determination.

3.4 Sensor potential response characteristics and lifespan

According to the IUPAC guidelines, the response time is known as the interval between adding the analyte to the sample solution and the time at which a limiting potential was reached. In this study, the response time was recorded by changing the DTZ concentrations in solution, over a concentration range 1.0×10^{-7} to 1.0×10^{-2} mol L^{-1}. The equilibrium response time is reached in 10 s, which indicates fast exchange kinetics of drug ions with ion exchanger at the surface of the paste. Repeatability and reproducibility are referred to the degree of agreement between the results of subsequent measurements of the same analyte, performed under specific conditions.[13]

The reversibility of a sensor which is the ability of the sensor to recover, or return to its original background/baseline condition was checked by recording the sensor response in the sequence high-to-low from 1.0×10^{-2} to 1.0×10^{-7} mol L^{-1}

sample concentrations of (DTZ) drug. The results showed that the response of the sensors was reversible (Fig. 7). These observations indicate no memory effect on the sensor response.

The repeatability of the measured potential of the sensor was tested by monitoring the measurement in 1.0×10^{-3} mol L^{-1} DTZ solution after measuring the first set of solutions at 1.0×10^{-4} mol L^{-1}. The RSD value of five reproducing measurements is 1.18% confirming the high precision of the sensor and demonstrating the absence of the memory effect. On the other hand, five independents sensors were prepared and tested in 1.0×10^{-5} mol L^{-1} DTZ solution to check the reproducibility. The sensor showed high reproducibility with RSD less than 1.9%.

The lifespan of the sensors was monitored by measuring the sensor performance at regular intervals. The received data indicated that the sensor was stable within 11 weeks.

3.5 Water layer test

It is well known that the presence of a water layer between the carbon paste and the transducer affects the sensor response,[34] which may cause O_2 or CO_2 to diffuse through the paste. While CO_2 can affect the pH of the interface, O_2 could favor redox side reactions. After conditioning in 1.0×10^{-3} mol L^{-1} DTZ solution, 1.0×10^{-3} mol L^{-1} verapamil hydrochloride interferent

Table 4 Application of the proposed sensor for the determination of DTZ in urine and industrial water samples

Statistical parameter	Taken mg	Urine		Industrial water	
		Recovery (%)	RSD (%)	Recovery (%)	RSD (%)
	0.023	97.65	1.16	97.96	0.86
	0.226	98.35	1.22	98.68	0.88
	22.55	99.50	1.19	99.45	0.78
Mean $\pm$ SD		98.50 $\pm$ 0.93		98.70 $\pm$ 0.75	

Table 5 Comparison of the proposed DTZ ion-selective method with published methods

Method	Linear range (mol L^{-1})	Detection limit (mol L^{-1})	Response time (s)	Applications	Reference
HPTLC	8.8×10^{-8} to 8.8×10^{-7}	4.4×10^{-8}	—	Bulk drug and pharmaceuticals	5
Spectrophotometric	—	1.10×10^{-4}	—	Commercial tablets and capsules	6
Cyclic voltammetry	2.0×10^{-6} to 8.0×10^{-5}	7.0×10^{-8}	—	Pharmaceutical formulation (capsule) and urine	8
PVC membrane	1.0×10^{-5} to 1.0×10^{-1}	7.09×10^{-6}	12	Pharmaceutical formulation and urine	10
DTZ-CPS	1.0×10^{-6} to 1.0×10^{-2}	5.0×10^{-7}	10	Urine and industrial water	P.W.[a]

[a] P.W.: present work.

solution was recorded and again in 1.0×10^{-3} mol L^{-1} DTZ solution. Fig. 8 indicated that, no potential deflection could be noticed, which shows that no water layer was identified. The high hydrophobicity of the carbon paste may be responsible for this behavior.

3.6 Effect of pH

The operational pH range of the constructed sensor was checked for 1.0×10^{-3} and 1.0×10^{-4} mol L^{-1} DTZ solutions over a wide pH range (1–12). The constructed sensor showed very slight potential fluctuations in a pH range of 2.0–8.0 (Fig. 9). The interference of the hydronium ion caused a drop in mV readings at lower pH levels (below pH 2.0). On the other hand, the development of non-protonated drug molecules may be the reason for the decrease in potential above pH 8.0.[35] This wide pH range provides the availability for DTZ ions detection in various matrices and is beneficial for routine work.

3.7 Effect of interference

The potentiometric sensor's selectivity behavior reflects the ability of the sensor to distinguish between analyte ions and other interfering species present in solution.[36] Therefore, the selectivity behavior is considered one of the most critical parameters which should be carefully checked. Traditional evaluation techniques, like the separate solution and matched potential methods,[37,38] are biased by the effects of the ion-exchange processes at the membrane/solution interface and transmembrane ions fluxes. Bakker protocol method is followed to check the selectivity behavior of the constructed sensor.[39] It depends on plotting calibration curves of the sensor potential against the logarithm of the interfering species concentrations. Calibration curves of different cations species (Na$^+$, K$^+$, Mg^{2+}, and Ca^{2+}) and a similar structural drug (verapamil) were plotted in order to investigate the ability of the examined sensor towards the selected interfering ions. As shown in Fig. 10, there is no significant response for all interfering species tested toward DTZ ion confirming the high selectivity of the investigated sensor. According to this protocol, the sensor potential is not distorted by either the ion exchange or the transmembrane flux at the membrane/solution interface.

3.8 Thermal stability

Over a temperature range of (15.0–60.0 °C), thermal stability of the constructed sensors was examined. The isothermal stability

coefficient value was found to be 0.00528 V per °C, indicating that the sensor has excellent thermal stability within the examined temperature range.

3.9 Analytical performance

Utilizing the standard addition and potentiometric titration methods, the validity of the examined sensor for quantitative analysis of DTZ was evaluated in pharmaceutical preparations, biological fluid (urine) and industrial water samples.

The constructed sensor was successfully applied as an indicator for potentiometric determination of 3–9 mL of 1.0×10^{-2} mol L^{-1} DTZ against 1.0×10^{-2} mol L^{-1} NaTPB solution as titrant. The obtained typical S-shaped plots and recoveries ranges indicate the applicability of the constructed sensor.

The standard addition method was applied for DTZ determination in the pure solution, pharmaceutical preparations, biological fluids (urine) and industrial water samples (Tables 3 and 4). The results listed in Table 3 showed good recovery (100.8 to 101.7) and small RSD. In addition, t- and F-tests were implemented and the values were less than the tabulated ones. It is clear that the fabricated sensor displayed a high precision and accuracy of the proposed methods.

3.10 Comparison with reported methods

The details of the comparison between the current work and previously published data are listed in Table 5. This suggested method has numerous benefits over other detection techniques, such as the linear range (1.0×10^{-6} to 1.0×10^{-2} mol L^{-1}) is wider than the reported data in Table 4 and the detection limit (5.0×10^{-7} mol L^{-1}) is lower than spectrophotometric[6] and potentiometric[10] techniques. Moreover, it is low cost, simple preparation and fast than the reported methods. The data listed in Table 5 illustrates that the sensor can be accurately and precisely determine DTZ in pure medications and pharmaceutical formulations.

4. Conclusion

In the current study, a highly sensitive, stable, and robust modified carbon paste sensor based on a new hybrid structures of ZnO@PANI/C nanocomposite was used for sensing DTZ. The constructed sensor showed high sensitivity towards DTZ with wide linear response range of 1.0×10^{-6} to 1.0×10^{-2} mol L^{-1},

excellent Nernstian slope of 62.0 $\pm$ 0.9 mV per decade, fast response time ($\leq$10 s) and wide pH range of 2.0–8.0. Attractively, the sensor has low detection limit of 5×10^{-7} mol L^{-1} and long lifespan of 11 weeks. The analytical application results in the present study showed that the sensors can be successfully applied in quality control laboratories for routine analysis of DTZ in pure form, ALTIAZEM® tablets, urine and industrial water samples.

Conflicts of interest

There are no conflicts to declare.

References

1 R. Ismail, N. H. Ismail, Z. Md Isa, A. Mohd Tamil, M. H. Ja'afar, N. Mat Nasir, S. Abdul-Razak, N. Zainol Abidin, N. H. Ab Razak, P. Joseph and K. H. Yusof, *Am. J. Med. Open*, 2023, **10**, 100049.

2 A. Gevaerd, F. R. Caetano, P. R. Oliveira, A. J. G. Zarbin, M. F. Bergamini and L. H. Marcolino-Junior, *Sens. Actuators, B*, 2015, **220**, 673–678.

3 N. Li, J. Wang, H. Han, L. Huang, F. Shao and X. Li, *Anal. Biochem.*, 2014, **447**, 90–97.

4 T. Alebić-Kolbah and F. Plavšić, *J. Pharm. Biomed. Anal.*, 1990, **8**, 915–918.

5 P. V. Devarajan and V. V. Dhavse, *J. Chromatogr. B: Biomed. Sci. Appl.*, 1998, **706**, 362–366.

6 N. Rahman and S. N. H. Azmi, *Microchem. J.*, 2000, **65**, 39–43.

7 M. Ghandour, E. Aboul Kasim, A. M. Ali, M. El-Haty and M. M. Ahmed, *J. Pharm. Biomed. Anal.*, 2001, **25**, 443–451.

8 S. Ostovar, S. Maghsoudi and M. Mousavi, *Synth. Met.*, 2021, **281**, 116928.

9 R. Imani, M. Shabani-Nooshabadi and N. Ziaie, *Chemosphere*, 2022, **297**, 134170.

10 M. R. Ganjali, T. Razavi, R. Dinarvand, S. Riahi and P. Norouz, *Int. J. Electrochem. Sci.*, 2008, **3**, 1543–1558.

11 M. M. Khalil, S. A. A. Moaty and M. A. Korany, *Sens. Actuators, B*, 2018, **273**, 429–438.

12 M. M. Khalil, A. A. Farghali, W. M. A. El Rouby and I. H. Abd-Elgawad, *Sci. Rep.*, 2020, **10**, 8607.

13 S. M. Mostafa, A. A. Farghali and M. M. Khalil, *Electroanalysis*, 2021, **33**, 1194–1204.

14 I. J. Gómez, M. V. Sulleiro, D. Mantione and N. Alegret, *Polymers*, 2021, **139**, 745, DOI: **10.3390/polym13050745**.

15 G. Liao, *Int. J. Chem.*, 2018, **10**, 81.

16 M. Beygisangchin, S. Abdul Rashid, S. Shafie, A. R. Sadrolhosseini and H. N. Lim, *Polymers*, 2021, **13**, 2003.

17 X. Yang, J. Wang, A. M. El-Sherbeeny, A. A. AlHammadi, W. H. Park and M. R. Abukhadra, *Chem. Eng. J.*, 2021, **431**, 134312.

18 S. N. Surip, A. S. Abdulhameed, Z. N. Garba, S. S. A. Syed-Hassan, K. Ismail and A. H. Jawad, *Surf. Interfaces*, 2020, **21**, 10064.

19 K. P. Flores, J. L. O. Omega, L. K. Cabatingan, A. W. Go, R. C. Agapay and Y. H. Ju, *Renewable Energy*, 2019, **130**, 510–523.

20 J. M. Fonseca, L. Spessato, A. L. Cazetta, K. C. Bedin, S. A. Melo, F. L. Souza and V. C. Almeida, *Energy Convers. Manage.*, 2020, **217**, 112975.

21 M. Shaban, M. R. Abukhadra, M. Rabia, Y. A. Elkader and M. R. Abd El-Halim, *Rend. Lincei Sci. Fis. Nat.*, 2018, **29**, 141–154.

22 M. R. Abukhadra, I. Saad, J. S. Khim, J. S. Ajarem and A. A. Allam, *Int. J. Environ. Anal. Chem.*, 2022, 1–21.

23 M. A. Sayed, M. R. Abukhadra, M. A. Salam, S. M. Yakout, A. A. Abdeltawab and M. A. Ibrahim, *Energy*, 2019, **187**, 115943.

24 Y. S. S. Sarma, N. Gupta and P. Bhattacharya, *Polym. Eng. Sci.*, 2022, **62**, 1918–1926.

25 R. Ismail, I. Šeděnková, J. Svoboda, M. Lukešová, Z. Walterová and E. Tomšík, *J. Mater. Chem. B*, 2023, **11**(7), 1545–1556.

26 I. G. Al-Labadi, M. H. Shemy, A. Y. Ghidan, A. A. Allam, H. M. Kálmán, J. S. Ajarem, J. Luo, C. Wang and M. R. Abukhadra, *Front. Chem.*, 2023, **11**, 1130682.

27 V. A. Mooss, F. Hamza, S. S. Zinjarde and A. A. Athawale, *Chem. Eng. J.*, 2019, **359**, 1400–1410.

28 W. Jiao, G. Ding, L. Wang, Y. Liu and T. Zhan, *Microchim. Acta*, 2022, **189**, 78.

29 H. Yu, S. Niu, T. Bai, X. Tang and C. Lu, *J. Cleaner Prod.*, 2018, **183**, 67–76.

30 C. Wang, J. Wang, L. Bai, R. Yang and H. Wang, *Materials*, 2019, **12**, 3550.

31 X.-Z. Li, S.-R. Liu and Y. Guo, *RSC Adv.*, 2016, **6**, 63099–63106.

32 C. Wardak, *Int. J. Environ. Anal. Chem.*, 2009, **89**, 735–748.

33 N. Gupta, R. K. Sahu, T. Mishra and P. Bhattacharya, *J. Mater. Chem. A*, 2022, **10**, 15794–15810.

34 N. Magdy, A. E. Sobaih, L. A. Hussein and A. M. Mahmoud, *Electroanalysis*, 2023, **35**(2), DOI: **10.1002/elan.202200119**.

35 E. Elgazzar, K. Attala, S. Abdel-Atty and A. M. Abdel-Raoof, *Talanta*, 2022, **242**, 123321.

36 K. A. Singh and S. Mehtab, *Sens. Actuators, B*, 2007, **123**, 429–436.

37 R. P. Buck and E. Lindner, *Pure Appl. Chem.*, 1994, **66**, 2527–2536.

38 Y. Umezawa, K. Umezawa and H. Sato, *Pure Appl. Chem.*, 1995, **67**, 507–518.

39 E. Bakker and E. Pretsch, *Anal. Chem.*, 2002, **74**, 420A–426A.